Backward Angle Anomaly in $^{9}Be+^{12}C$ Scattering. I*

Shigeo OHKUBO**
Department of Applied Science,
Kochi Women's University
Kochi 780, Japan

(Received 22 November 1980)

Abstract: It is shown that a parity dependent potential model successfully explains the backward angle anomaly in $^{9}Be+^{12}C$ elastic scattering over a wide range of energy. A mechanism of enhancement of cross sections at backward angles is systematically studied.

§1. Introduction

In heavy ion scattering anomalous enhancement of cross sections at backward angles occurs in a wide range of mass and energy. This phenomenon of backward angle anomaly (BAA) arises especially for heavy ion scattering in which mass difference between projectile and target is small.[1] Recently it has been shown that BAA also appears in $^{9}Be+^{12}C$ scattering in a wide energy region.[2-6] This anomaly has not been explained by the usual optical potential model. In a separate paper[7] we have shown that BAA can be successfully explained by the parity dependent potential model, which has been proposed based on the exchange effect due to the Pauli principle.[8-9]

The parity dependent potential model is expressed by

$$V(r)=V_{opt}(r)+(-)^{l}V_{exch}(r), \tag{1}$$

where

$$V_{opt}(r)=-V_0 f(a,r_0;r)-iW_0 f(a_I,r_I;r)+V_c(r), \tag{2}$$

and

$$V_{exch}(r)=4V_\pi a_\pi \frac{d}{dr} f(a_\pi,r_\pi;r). \tag{3}$$

The function $f(a, r_o; r)$ is Woods-Saxon volume type and the Coulomb potential V_c is assumed to be of a uniformly charged sphere.

The purpose of the present paper is to investigate a mechanism of enhancement of cross sections at backward angles with use of a parity dependent potential model through a systematic analysis of the experimental data. In the next section properties of the parity dependent potential model is quantitatively studied and analysis of the experimental data is presented in §3, where sign of the parity dependent potential is also briefly discussed. Concluding remarks are given in §4.

---

*) A preliminary report is given in *Proceedings of the International Conference on Nuclear Physics*, (Berkeley, 1980), p. 477.

**) Present address: Research Institute for Fundamental Physics, Kyoto University, Kyoto 606, Japan

§2. Properties of the parity dependent potential model

We investigate a role of the parity dependent potential for angular distributions at backward angles in $^{9}Be+^{12}C$ scattering. The calculated angular distributions at $E_{Lab}=39.68$ MeV are shown in Fig. 1 for the cases of $V_{\pi}=0$, 0.2, 0.6, 1.0 and 3.0 MeV. Here only

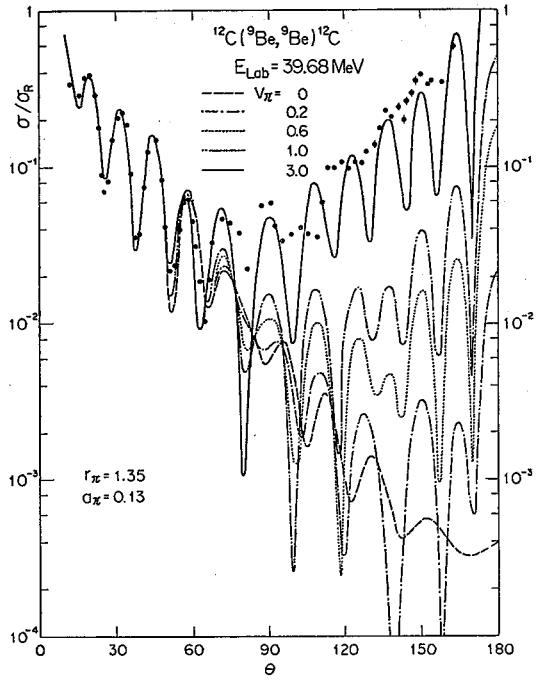

Fig. 1. A dependence on V_{π} of the calculated angular distributions in $^{9}Be+^{12}C$ scattering is shown at $E_{Lab}=39.68$ MeV. The dashed, dash-dotted, dotted, dash-two-dotted and solid lines represent the angular distributions calculated with our model in the cases of $V_{\pi}=0$, 0.2, 0.6, 1.0 and 3.0 MeV, respectively. The potential parameters of V_{opt} are $V_0=33.686$, $r_0=0.964$, $a=0.921$, $W_0=6.524$, $r_I=1.509$, $a_I=0.478$ and $r_c=1.45$, respectively.

the strength parameter V_{π} of the parity dependent potential is varied and the other potential parameters are fixed. It is clearly seen that the cross sections at backward angles are strongly enhanced by the parity dependent potential. The backward angular distributions rise step by step as V_{π} increases, while the forward angular distributions are scarcely changed. It is noted that even a small parity dependence causes enhancement of cross sections and oscillations at backward angles.

In order to see a mechanism of enhancement of cross sections we analyze the scattering amplitude at backward angles. In Fig. 2 total scattering amplitude $f(\theta=180°)$ including Coulomb scattering amplitude at an extreme back-angle $\theta=180°$ is shown for various cases of V_{π} values. All the scattering amplitudes $f(\theta=180°)$ plotted are on a straight line. As V_{π} increases the vector of scattering amplitude linearly increases. These properties are reasonably understood by considering that the parity dependent potential can be treated as a perturbation to the parity independent potential V_{opt}[7], which shows that $f(\theta=180°)$ is

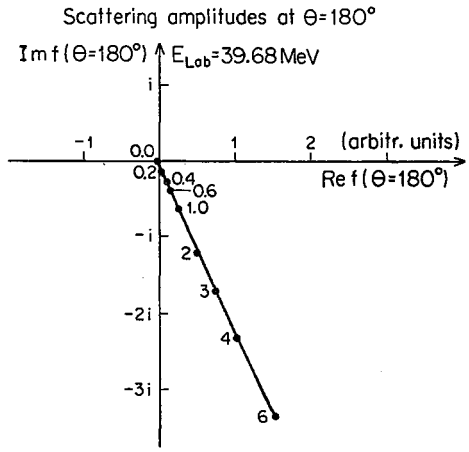

Fig. 2. The total scattering amplitudes $f(\theta=180°)$ at $\theta=180°$ including Coulomb scattering amplitude are shown for various V_π values. The $f(\theta=180°)$ is shown by the points and the value of V_π is indicated by the figure. The straight line connecting the points is drawn to guide eyes.

linearly dependent on V_π. It is quite interesting to note that even the scattering amplitude $f(\theta=180°)$ for $V_\pi=6$ MeV is on the straight line. Treatment of V_π in the perturbation seems valid for quite a large parity dependence. In Fig. 3 the total scattering amplitude $f(\theta=180°)$ is given as a vector sum of each partial wave scattering amplitude. Although each partial scattering amplitude is large itself, the adjacent even-odd partial scattering

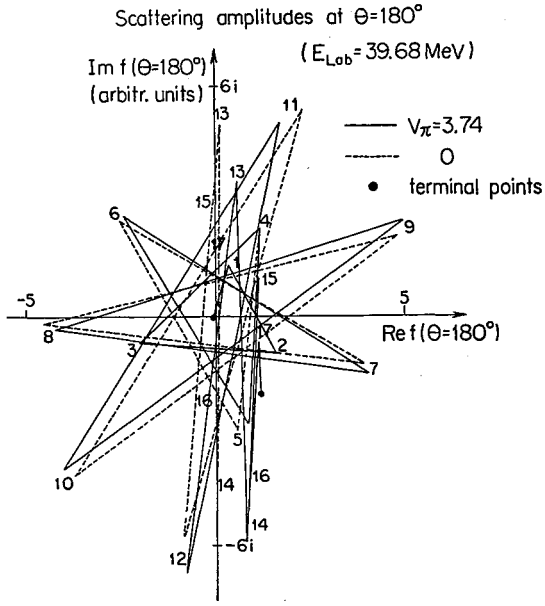

Fig. 3. The total scattering amplitudes $f(\theta=180°)$ at $\theta=180°$ are shown as a vector sum of the partial wave scattering amplitudes. The solid and dashed lines represent the partial wave scattering amplitude for $V_\pi=3.74$ MeV and $V_\pi=0$ MeV, respectively. The orbital angular momentum of the partial wave is indicated by figure. Net scattering amplitudes are indicated by the black circles.

amplitudes almost cancel out each other to give a rather small net scattering amplitude. In the case of the parity dependent potential this cancellation is slightly weakened, especially for surface partial waves and a net scattering amplitude $f(\theta=180°)$ becomes about factor seven as large as that of $V_\pi=0$ case. The scattering amplitude caused by the parity dependent potential is essential for making a net scattering amplitude great. This is seen in Fig. 4, where the difference of the scattering amplitudes for $V_\pi=3.74$ and for $V_\pi=0$,

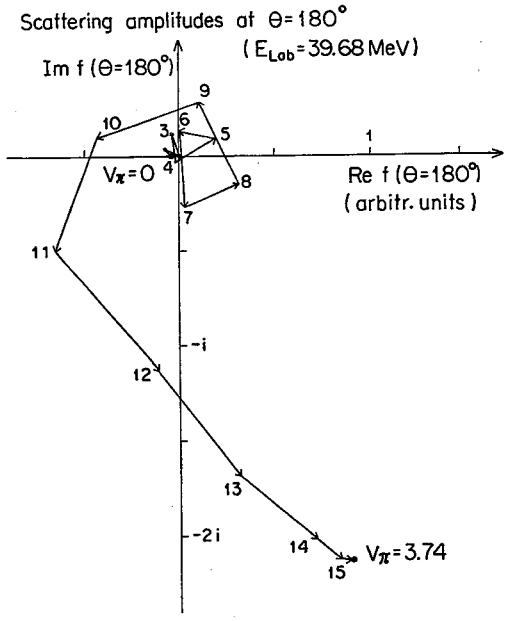

Fig. 4. The difference of the scattering amplitude between $f(\theta=180°)$ for $V_\pi=3.74$ MeV and $f(\theta=180°)$ for $V_\pi=0$ MeV is shown dividing into the vectors of the partial wave scattering amplitudes. Each line represents the partial wave scattering amplitude of which angular momentum is indicated by a figure at a terminal point of the vector. The total scattering amplitudes $f(\theta=180°)$ for $V_\pi=3.74$ MeV and 0 MeV are indicated by the black circles.

that is the scattering amplitude due to the parity dependent potential, is shown dividing into each partial wave scattering amplitude. It is found that the partial scattering amplitudes for surface partial waves caused by the parity dependent potential are not only large compared with low partial waves but also summed up coherently to give a significantly large net scattering amplitude. This is the reason why the scattering amplitude at backward angles is strongly enhanced by the parity dependent potential. The coherent sum of the partial wave scattering amplitudes caused by the parity dependent potential comes from the even-odd feature of the scattering matrix. The reflection coefficient is shown in Fig. 5. The even-odd staggering appears for the surface partial waves in the case of the parity dependent potential compared with the $V_\pi=0$ case. Although this even-odd staggering is small, its contribution to the scattering amplitude at backward angles is great. The contribution of the lower partial waves to the total scattering amplitude is not important. Thus, it is found that the parity dependent potential is essentially responsible for enhancement of cross sections at backward angles. It is further noted that the backward enhancement is

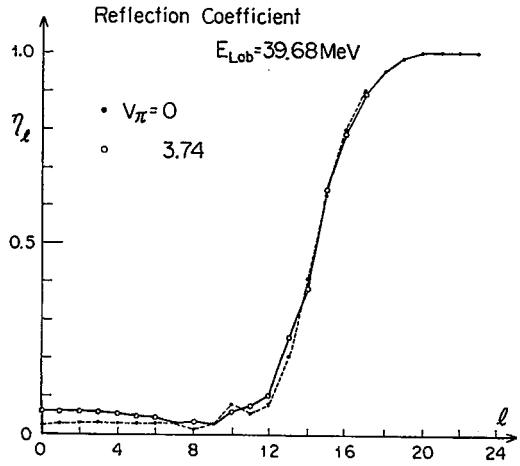

Fig. 5. Reflection coefficients η_l as a function of the orbital angular momentum. The white circles calculated by the parity dependent potential with V_π=3.74 MeV are jointed by the solid lines and black circles by the usual optical potential model with V_π=0 MeV are depicted by the dashed lines.

not due to a single partial wave, such as a resonance, but due to some surface partial waves.

§ 3. Analysis of the experimental data

We analyze the anomalous angular distributions with our model. Since the parity dependent potential is responsible for the backward enhancement of cross sections, we adjust

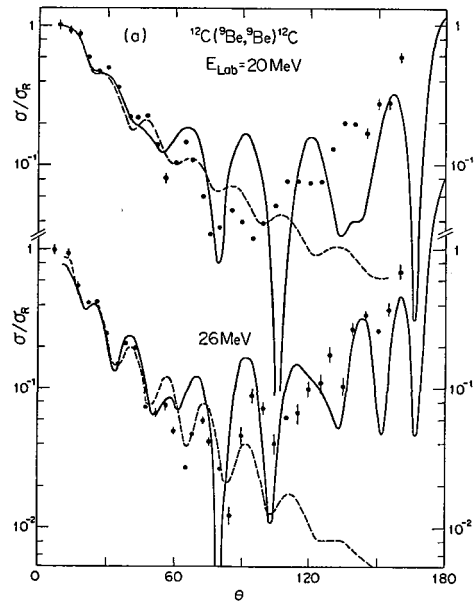

Fig. 6 (to be continued)

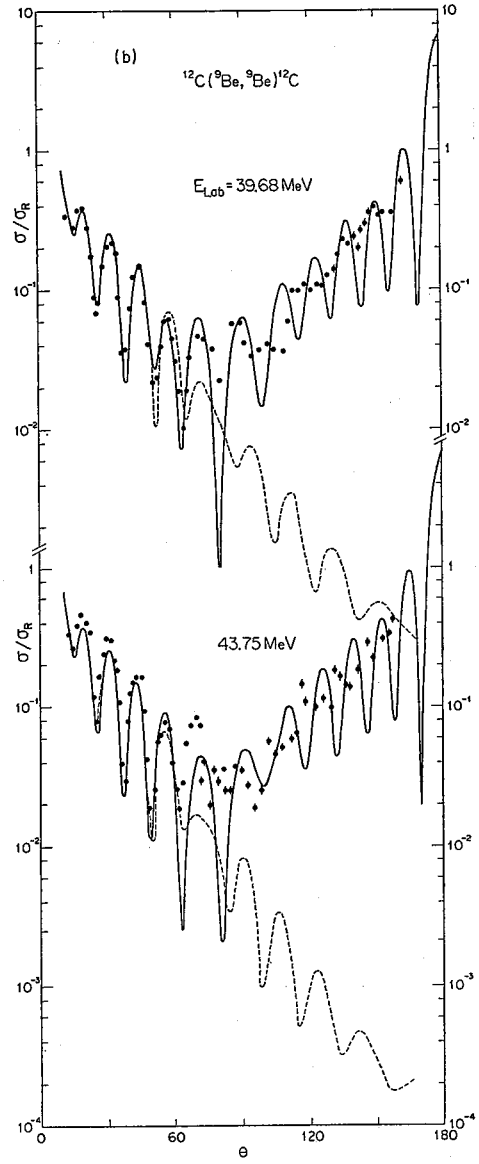

Fig. 6. Angular distributions of $^{9}Be+^{12}C$ scattering at E_{Lab}=20, 26, 39.68 and 43.75 MeV. The points represents the experimental data.[3,6] The solid and dashed lines are calculated with the parity dependent potential model and with the usual optical potential model of $V_{\pi}=0$, respectively. The parity dependent potential parameters are listed in Table I and those for V_{opt} are given in caption of Fig. 1.

Table I. Parameters of the parity dependent potential. Other potential parameters of the parity independent potential V_{opt} are shown in caption of Fig. 1.

E_{Lab} (MeV)	V_π (MeV)	r_π (fm)	a_π (fm)
20	7.53	1.350	0.13
26	6.27	1.350	0.13
39.68	3.67	1.350	0.13
43.75	2.99	1.350	0.13

only the parity dependent potential parameters while the parity independent potential V_{opt} is fixed to the one determined by Mateja et al.[6] First we try to fit the data by adjusting only one parameter V_π, with the other two parameters r_π and a_π fixed to 1.350 and 0.13, respectively. This radius parameter is considerably larger than that of real potential. The calculated angular distributions for E_{Lab}=20, 26, 39.68 and 43.75 MeV are shown in Fig. 6 and the potential parameters are listed in Table I. The cross sections at backward angles are greatly enhanced by the parity dependent potential and the agreement with the experimental data is improved much. The usual optical potential model calculations with V_π=0 decrease toward large angles and a few orders of magnitude smaller than the experimental data. The fit to the data at backward angles is not satisfactory at lower energies, especially for E_{Lab}=20 MeV. For E_{Lab}=20 MeV at around $\theta\sim140°$ the calculated angular distribution shows a valley in contradiction to the data. Further at intermediate angles the fit to the data is not so good. For E_{Lab}=26 MeV the fit is better than that for E_{Lab}=20 MeV. At intermediate angles, however, peaks of the angular distribution deviate slightly from the data. This insufficiency may be removed by adjusting the remained parity dependent potential parameters. For the higher energies of 39.68 and 43.75 MeV the small diffuseness parameter is preferred to fit the data but for the lower energies this value may not be appropriate. In the analyses the parity dependence decreases as energy increases. This is reasonable from the viewpoint of the Pauli principle since the exchange effect becomes smaller at higher energies.

In order to improve a fitting for the lower energies diffuseness parameter is varied in addition to V_π. When only a_π is varied with V_π fixed at the obtained value in Table I a significant improvement is not attained. So the best fit parameters are searched by varying both V_π and a_π independently starting from the initial value in Table I. The obtained angular distributions for E_{Lab}=20 and 26 MeV are shown in Fig. 7. The fit to the data is significantly improved. It is noted that diffuseness parameter a_π has increased much while contrary V_π has become small much. Increase of a_π compensates decrease of V_π. For lower energies parity dependent potential seems to be effective in a wider range than for higher energies.

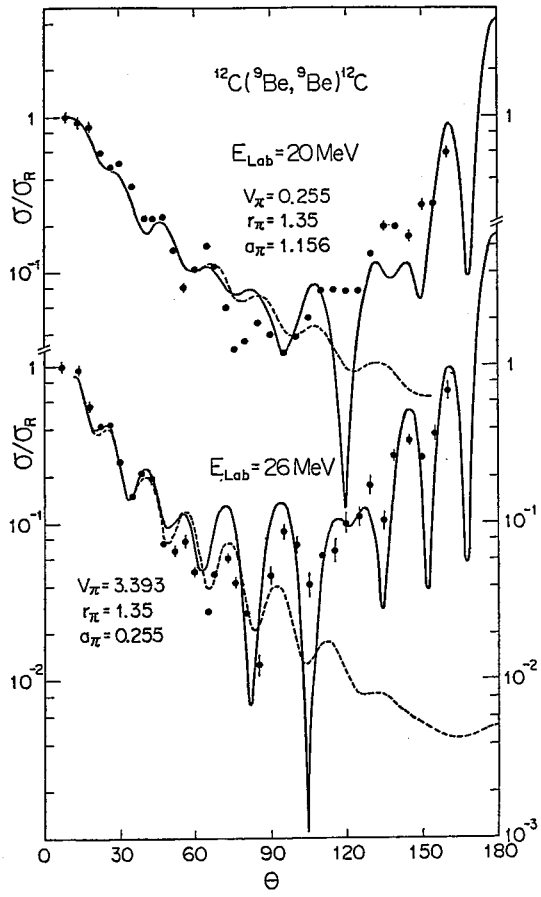

Fig. 7. Angular distributions of $^{9}Be+^{12}C$ scattering at E_{Lab}=20 and 26 MeV. The solid and dashed lines represent the parity dependent potential model calculations and the usual optical model calculations, respectively.

If we vary all the three parameters freely the fit to the data is of course improved. The obtained angular distributions are shown in Fig. 8 and the parity dependent potential parameters are listed in Table II. For E_{Lab}=20 and 26 MeV agreement with the data is further improved. The parity dependent potential appears even at rather inner region as the strength V_π has become quite large. The parity dependent potential at the surface region is effective even if it is small. The potential parameter set is not unique and there will be other parameter sets which give a comparable fitting.

Through the systematic analyses it is found that the parity dependent potential reproduces well the anomalous backward rise.

Next we discuss the sign of the parity dependent potential. In the sense of Baye et al.[10] the potential for $^{9}Be+^{12}C$ scattering seems deeper for even parity than for odd one, i. e. $V_\pi>0$. Although in the analyses we adopted $V_\pi>0$, it is not self-evident in the framework of the model. In fact backward rise is obtained in the case of $V_\pi<0$. In Fig. 9 we show the calculated angular distributions at E_{Lab}=26 MeV for the cases of V_π=0, −2, −4 and −8 MeV. As absolute value of V_π increases, the magnitude of backward

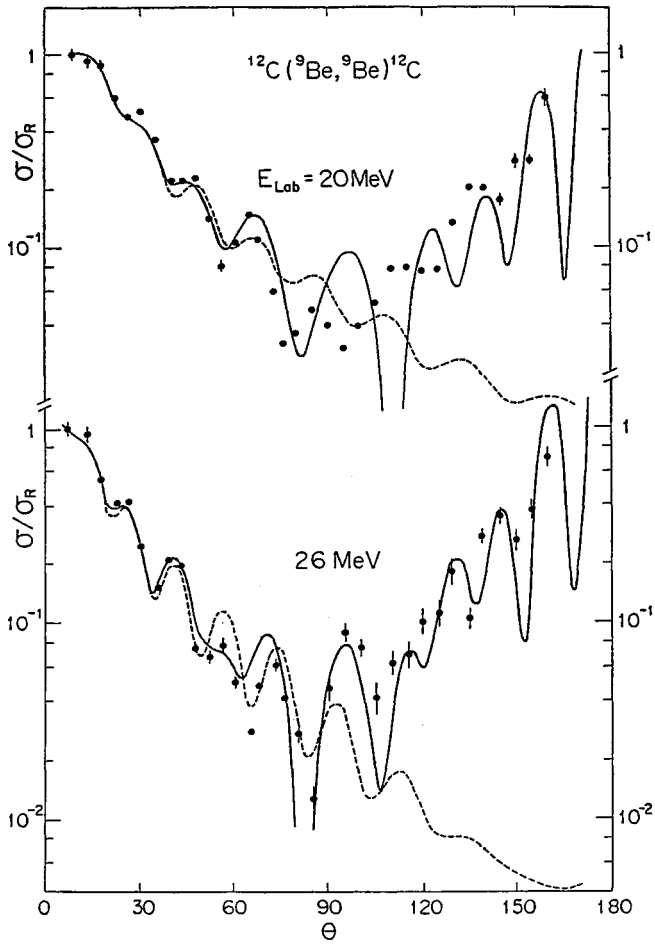

Fig. 8. Angular distributions of $^{9}Be+^{12}C$ scattering at E_{Lab}=20 and 26 MeV, respectively. This figure is taken from Ref. 7). The solid lines represent the parity dependent potential model calculations and the dashed lines represent the usual optical model calculations. The potential parameters are shown in Table II.

Table II. Parameters of the parity dependent potential. Other potential parameters of the parity independent potential V_{opt} are shown in caption of Fig. 1.

E_{Lab} (MeV)	V_π (MeV)	r_π (fm)	a_π (fm)
20	11.55	1.154	0.482
26	10.20	1.233	0.377
39.68	3.74	1.349	0.128
43.75	3.22	1.355	0.113

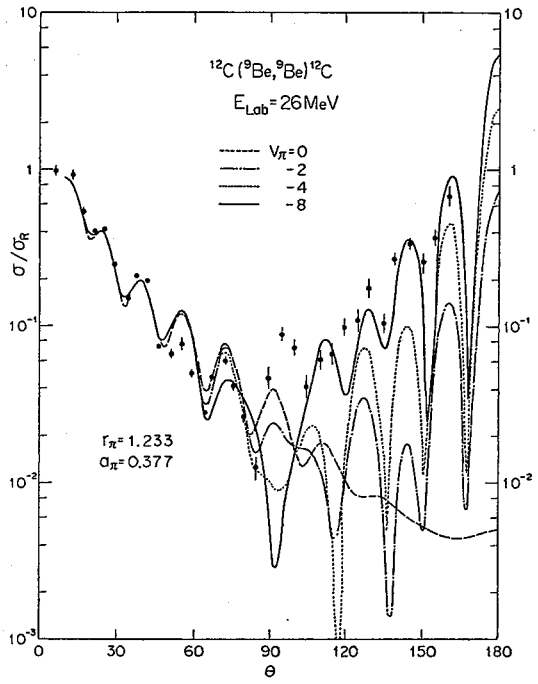

Fig. 9. V_π-dependence of the angular distributions at E_{Lab}=26 MeV is shown for the negative V_π values. Potential parameters are the same as those in Table II except for V_π. The dashed, dash-dotted, dotted and solid lines represent the angular distributions calculated with our model in the cases of V_π=0, −2, −4 and −8 MeV, respectively.

cross sections is enhanced. This trend is the same as seen in the case of $V_\pi>0$ in Fig 1. The properties of the parity dependent potential model discussed in §2 are also true for the case of negative V_π value. The experimental data of backward angle anomaly can be well reproduced with the negative V_π. Although there appears a difference in the angular distributions at the intermediate angular region from $V_\pi>0$ case, it seems difficult to determine the sign of V_π within the framework of the present model. An important thing is that parity dependence of the potential should exist in the surface region.

§4. Concluding remarks

We have studied BAA in $^{9}Be+^{12}C$ scattering with use of the parity dependent potential model. Systematic analyses have shown that the parity dependent potential model satisfactorily reproduces the anomalous angular distributions. It has been found that enhancement of cross sections at backward angles is brought about by a coherent sum of the partial scattering amplitudes for surface partial waves which are caused by the parity dependent potential. Although we have analyzed the data with $V_\pi>0$ potential, it has been made clear that $V_\pi<0$ can reproduce the backward rise as well. It will be necessary to study further the sign of V_π in detail.

We have used the surface type for the parity dependent potential, since it is considered

to be effective at surface region. At lower energies, however, parity dependence at the rather inner region is needed. It is interesting to study BAA with the parity dependent potential of volume type.

Acknowledgements

The author thanks Professor T. Ando for his interest and continuous encouragement. Numerical calculations were carried out on the computer systems of FACOM M200 at the Data Processing Center of Kyoto University and ACOS-900 of Osaka University.

1) W. Von Oeretzen: Phys. Reports 19C, 1 (1975). See also references therein.
2) P.H. Barker, A. Huber, H. Knoth, U. Matter, A. Gobbi and P. Marmier: Nucl. Phys. A155, 401 (1975).
3) J. Lang, R. Müller, E. Ungricht, L. Jarczyk, J. Okolowicz and A. Strzalkowski: *Proceedings of the International Conference on Clustering Aspects of Nuclear Structure and Nuclear Reactions*, edited by W.T.H. Van Oers (AIP, New York, 1978), p. 682.
4) E. Ungricht, D. Balzer, M. Hugi, J. Lang and R. Müller: Nucl. Phys. A313, 376 (1979).
5) L. Jarczyk, J. Okolowicz, A. Strzalkowski, K. Bodek, M. Hugi, J. Lang, R. Müller and E. Ungricht : Nucl. Phys. A316, 139 (1979).
6) J.F. Mateja, A.D. Frawley, P.B. Nagel and L.A. Parks: Phys. Rev. C20, 176 (1979).
7) S. Ohkubo: to be published.
8) Y. Kondo, S. Nagata, S. Ohkubo and O. Tanimura: Prog. Theor. Phys. 53, 1006 (1975).
9) S. Ohkubo: Phys. Rev. C22, 36 (1980).
S. Ohkubo: *Proceedings of the International Conference on Nuclear Physics*, (Berkeley, 1980), p. 444.
S. Ohkubo: *Proceedings of the International Symposium on Highly Excited State in Nuclear Reactions*, (Osaka, 1980), p. 104.
10) D. Baye, J. Deenen and Y. Salmon: Nucl. Phys. A289, 511 (1977).